Molecular Vision 2021; 27:191-205 <http://www.molvis.org/molvis/v27/191>
Received 26 February 2020 | Accepted 26 April 2021 | Published 28 April 2021

Differences in activation of intracellular signaling in primary human retinal endothelial cells between isoforms of VEGFA 165

Wendelin Dailey, Roberto Shunemann, Fang Yang, Megan Moore, Austen Knapp, Peter Chen, Mrinalini Deshpande, Brandon Metcalf, Quentin Tompkins, Alvaro E. Guzman, Jennifer Felisky, Kenneth P. Mitton

Eye Research Institute, Oakland University, Rochester, MI

Purpose: There are reports that a b-isoform of vascular endothelial growth factor-A 165 ($VEGFA_{165}$b) is predominant in normal human vitreous, switching to the a-isoform ($VEGFA_{165}$a) in the vitreous of some diseased eyes. Although these isoforms appear to have a different ability to activate the VEGF receptor 2 (VEGFR2) in various endothelial cells, the nature of their ability to activate intracellular signaling pathways is not fully characterized, especially in retinal endothelial cells. We determined their activation potential for two key intracellular signaling pathways (MAPK, AKT) over complete dose–response curves and compared potential effects on the expression of several $VEGFA_{165}$ target genes in primary human retinal microvascular endothelial cells (HRMECs).

Methods: To determine full dose–response curves for the activation of MAPK (ERK1/2), AKT, and VEGFR2, direct in-cell western assays were developed using primary HRMECs. Potential differences in dose–response effects on gene expression markers related to endothelial cell and leukocyte adhesion (*ICAM1*, *VCAM1*, and *SELE*) and tight junctions (*CLDN5* and *OCLN*) were tested with quantitative PCR.

Results: Activation dose–response analysis revealed much stronger activation of MAPK, AKT, and VEGFR2 by the a-isoform at lower doses. MAPK activation in primary HRMECs displayed a sigmoidal dose–response to a range of $VEGFA_{165}$a concentrations spanning 10–250 pM, which shifted higher into the 100–5,000 pM range with $VEGFA_{165}$b. Similar maximum activation of MAPK was achieved by both isoforms at high concentrations. Maximum activation of AKT by $VEGFA_{165}$b was only half of the maximum activation from $VEGFA_{165}$a. At a lower intermediate dose, where $VEGFA_{165}$a activated intracellular signaling stronger than $VEGFA_{165}$b, the changes in VEGFA target gene expression were generally greater with $VEGFA_{165}$a.

Conclusions: In primary HRMECs, $VEGFA_{165}$a could maximally activate MAPK and AKT at lower concentrations where $VEGFA_{165}$b had relatively little effect. The timing for maximum activation of MAPK was similar for the isoforms, which is different from that reported for non-retinal endothelial cells. Although differences in $VEGFA_{165}$a and $VEGFA_{165}$b are limited to the sequence of their six C-terminal six amino acids, this results in a large difference in their ability to activate at least two key intracellular signaling pathways and VEGF–target gene expression in primary human retinal endothelial cells.

Vascular endothelial growth factor-A 165 ($VEGFA_{165}$) is the isoform of VEGF that is primarily responsible for driving retinal vascular pathology in diabetic retinopathy (DR), age-related macular degeneration (AMD), and retinopathy of prematurity (ROP), through activation of VEGF receptor 2 (VEGFR2). A seminal analysis of the vitreous fluids of patients with diabetic retinopathy established the presence of elevated VEGF concentrations associated with this and other conditions [1]. That study contributed to the eventual development of intravitreal VEGF-blocking drugs to treat neovascularization and edema in AMD and DR, and the current exploration of their use for ROP [3-5].

Blockade of VEGFA activity is provided by the use of intravitreal drugs, including ranibizumab (Lucentis, Genentech), bevacizumab (Avastin, Genentech), pegaptanib (Macugen, Bausch & Lomb), and aflibercept (Eylea, Regeneron). Some VEGF-blocking drugs injected into the vitreous can enter the systemic circulation, and in the case of bevicizumab and aflibercept, they can substantially decrease serum VEGF concentration for several days [6]. There is interest in advancing VEGF-regulating therapies through more precise titration of the VEGF concentration or modulating specific VEGF-mediated signaling rather than the full blockade provided by current drugs. This field will continue to benefit from more complete knowledge of VEGF's signaling mechanisms within retinal endothelial cells. Unfortunately, much previous VEGF research did not technically differentiate

Correspondence to: Kenneth P. Mitton, Eye Research Institute, Oakland University, Rochester MI; FAX: (248) 370-4211; Phone: (248) 370-2079; email: mitton@oakland.edu
Dr. Shunemann now at Clinica Opthtalmus, Joinville – SC, Brazil
Dr. Yang now at Department of Ophthalmology, Renmin Hospital, Hubei University of Medicine, Shiyan, Hubei, P.R. China
Dr. Knapp now at Cleveland Clinic Cole Eye Institute, Cleveland OH
Dr. Chen is now at Department of Ophthalmology, University of Cincinnati, Cincinnati OH

between the VEGFA isoforms, and in the case of the retina, there is far less investigation using retinal endothelial cells, and even less from the human retina.

In addition to endothelial cells, VEGF receptors are expressed by cells of the immune system, including early and late hematopoietic progenitor cells, dendritic cells, T-lymphocytes, and macrophages [7]. Among the three VEGF receptor tyrosine-kinases (R1, R2, R3), VEGFR2 is required for angiogenesis and vasculogenesis, and its expression is most abundant in endothelial and endothelial progenitor cells [8-10]. VEGFR2 binds several isoforms of VEGFA that are produced from alternative splicing [11-14]. The most frequently detected isoforms are $VEGFA_{121}$, $VEGFA_{165}$, and $VEGFA_{189}$, with 121, 165, and 189 amino acids, respectively. $VEGFA_{121}$ is most diffusible, lacking the heparin-binding domains of $VEGFA_{165}$ and $VEGFA_{189}$. $VEGFA_{189}$ has even more affinity for heparin than $VEGFA_{165}$ with an additional heparin-binding domain encoded by exon 6 [11,12]. $VEGFA_{165}$ binds as a dimer to activate VEGFR2, and binds neuropilin 1 as a coreceptor. $VEGFA_{121}$ lacks two regions required to bind neuropilin 1.

The vast knowledge of VEGF-mediated signaling is mostly derived from the study of non-retinal cell types, and is beyond the scope of this paper; however, readers can refer to the excellent review by Koch and Claesson-Welch [15]. In endothelial cells, several pathways are activated by $VEGFA_{165}$ that affect proliferation, migration, survival, and endothelial permeability. Two of these pathways include MAPK (ERK1/2) and AKT (PKB), where MAPK is a dominant regulator of cell proliferation, and AKT modulates cell survival and permeability [16-19]. Autophosphorylation of VEGFR2 (Y1175) leads to RAS-independent activation of the phospholipase-C□ (PLC□)/protein kinase C/MAPK pathway [20,21]. Activation of VEGFR2 also leads to activation of the TSAD/phosphotidylinositol-3 kinase (PI3K)/phosphoinositide-dependent protein kinase (PDK)/AKT pathway [22,23]. AKT phosphorylates the BCL-2-associated death protein (BAB) and caspase-9 to block apoptosis and increase EC survival [24]. AKT also activates endothelial nitric oxide synthase eNOS (*NOS3*; Gene ID 4846, OMIM 163729) to modulate vascular permeability [25].

Recently, b-isoforms of VEGFA were described that differ from the previously known a-isoforms in the sequence of their C-terminal six amino acids: CDKPRR in $VEGFA_{165}$a becomes SLTRKD in $VEGFA_{165}$b [13,14]. This difference renders $VEGFA_{165}$b incapable of bringing neuropilin 1 into a receptor–ligand complex with VEGFR2 [26-28]. Similar to $VEGFA_{121}$, $VEGFA_{165}$b is reported to be less angiogenic than $VEGFA_{165}$a [13,29,30]. $VEGFA_{165}$b's binding affinity for VEGFR2 itself is similar to that of $VEGFA_{165}$a in human umbilical vein endothelial cells (HUVECs) and less than $VEGFA_{165}$a in direct binding analysis in transformed human embryonic kidney cells 293 (HEK293) cell assays [31,32]. $VEGFA_{165}$b also displays weaker activation of VEGFR2 and ERK1/2 (MAPK) than $VEGFA_{165}$a in transfected porcine aortic endothelial (PAE) cells [31]. Perrin et al. reported a switch from mostly $VEGFA_{165}$b to mostly $VEGFA_{165}$a in the vitreous of patients with active diabetic retinopathy [33]. A similar shift, from $VEGFA_{165}$b to $VEGFA_{165}$a, was reported in vitreous humor from young patients with ROP [34]. A murine equivalent of isoform switching ($VEGFA_{164}$b to $VEGFA_{164}$a) was also reported in a mouse model of oxygen-induced retinopathy [35]. Several publications using isoform-specific antibodies have detected $VEGFA_{165}$b in human and mouse tissues, but their presence from RNA analysis in sheep hypothalamus is controversial [36].

Although single-dose studies using transfected cells or non-retinal endothelial cells indicate that $VEGFA_{165}$b activates VEGFR2 and MAPK less than $VEGFA_{165}$a, we do not know if this is true throughout a full dose range. We also wanted to determine full dose–response curves for activation of intracellular signaling in primary human retinal microvascular endothelial cells. We hypothesized that there is a significant difference in the full dose–response curves for activation of these pathways in human retinal endothelial cells between $VEGFA_{165}$a and $VEGFA_{165}$b. To address this, we used in situ assays to determined full dose–response curves for the activation of MAPK (ERK1/2), AKT, and VEGFR2 in primary HRMECs for $VEGFA_{165}$a and $VEGFA_{165}$b. The results demonstrate that there is a significant dose–response difference in the ability of these two isoforms to activate intracellular signaling kinases, and that these dose–response differences propagate to differences in VEGF–target gene expression in primary human retinal endothelial cells.

METHODS

Certification of primary human retinal microvascular endothelial cells: Primary human retinal microvascular endothelial cells (HRMECs, genotype XY) were obtained from Cell Systems (Kirkland, WA) as passage 3 cells (catalog number: ACBRI-181). Cells used for experimentation were not used past passage 7. The endothelial character of the cell line was established by Cell Systems immunofluorescence testing: >95% positive by immunofluorescence for cytoplasmic VWF/Factor VIII, cytoplasmic uptake of Di-I-Ac-LDL, cytoplasmic CD31, and <1% by immunofluorescence for glial fibrillary acidic protein (GFAP), glutamine synthetase, neural/glial antigen 2 (NG2), and platelet-derived growth factor receptor

Table 1. Specific antibodies used and sources.

Antibody	IgG Species	Company	Cat. No.
Phospho-AKT (P-Ser473)	Rabbit	Cell Signaling Technologies	4058
AKT(pan)	Rabbit	Cell Signaling Technologies	4691
Phospho-p44/42 MAPK (Thr202/204)	Rabbit	Cell Signaling Technologies	4370
p44/42 MAPK (pan)	Rabbit	Cell Signaling Technologies	4695
Phospho-VEGFR2 (Tyr1175)	Rabbit	Cell Signaling Technologies	2478
Beta-Actin	Mouse	Millipore	MAB1501
Anti-mouse IgG IRDye 800CW	Goat	LI-COR	32,210
Anti-rabbit IgG IRDye 680RD	Goat	LI-COR	68,071
Anti-rabbit IgG IRDye 800CW	Goat	LI-COR	32,211
Anti-mouse IgG IRDye 680RD	Goat	LI-COR	68,070

beta (PDGFR-beta). The cell line was also subjected to short tandem repeat (STR) profile testing by cell systems at the master level (P1), performed by the laboratory analysis service of the American Type Culture Collection (ATCC, Manassas, VA). Seventeen STR loci plus the gender-determining locus, amelogenin, were amplified using the commercially available PowerPlex® 18D Kit from Promega. The cell line sample was processed using the ABI Prism® 3500xl Genetic Analyzer. Data were analyzed using the GeneMapper® IDX v1.2 software (Applied Biosystems). Appropriate positive and negative controls were used throughout the test procedure. The DNA profile (STR #12625 Analysis) was as follows: TH01: 9, 9.3; D5S818: 9, 13; D13S317: 8, 10; D7S820: 11, 12; D16S539: 11, 12; CSF1PO: 10, 12; Amelogenin: X, Y; vWA: 16, 19; TPOX: 8, 11. The ATCC test conclusions were that the submitted sample profile is human, but not a match to any profile in the ATCC STR database, as would be expected for primary HRMECs. Additionally, routine testing for retinal endothelial character at the author's laboratory (Eye Research Institute, Oakland University) confirmed that the HRMECs express all three of the human Norrin receptor-complex genes *FZD4* (Gene ID 8322, OMIM 604579), *LRP5* (Gene ID 4041, OMIM 603506), and *TSPAN12* (Gene ID 23,554, OMIM 613138), using real-time PCR analysis (data not shown). The HRMECs also demonstrated VEGF-mediated regulation of several VEGF target genes, as shown in the results.

Cell culture and antibodies: The EndoGRO-MV Complete Media Kit for culture of microvascular endothelial cells without VEGF was obtained from Millipore (Burlington, MA). EndoGro basal medium was supplemented with rhEGF, L-glutamine, heparin sulfate, and ascorbic acid according to the kit instructions. Additionally, supplementation with fetal bovine serum (FBS) and hydrocortisone hemisuccinate (1 µg/ml) was dependent upon the assay requirements. Recombinant human $VEGFA_{165}$a and $VEGFA_{165}$b were obtained from R&D Systems (Minneapolis, MN). Odyssey Blocking Buffer and an Odyssey Infrared Imager were purchased from LI-COR Biosciences (Lincoln, NE). The antibodies used for in situ labeling of HRMECs (in-cell western, ICW) and western blotting are summarized in Table 1. Mini Protean TGX gels were purchased from Bio-Rad (Hercules, CA).

Immunoblotting of activated MAPK and AKT in HRMECs: HRMECs were grown in 100 mm dishes that had been precoated with attachment factor (Cell Systems, Kirkland, WA). The medium was EndoGRO (No VEGF, Millipore Sigma, Burlington, MA) with 5% FBS to establish confluency. When the cells were confluent, the media were replaced with fresh media with or without $VEGFA_{165}$ isoforms. After incubation for 10 min, the cells were washed with ice-cold PBS (1X; 9.8 mM Na2HPO4, 2.5 mM NaH2PO4, 137 mM NaCl, 2.7 mM KCl, pH 7.4, Fisher Scientific, Pittsburg PA), and the dishes were scraped to detach the cells. The cell suspension was centrifuged at 1,000 × *g* for 5 min, and the cells were reconstituted in radioimmunoprecipitation assay (RIPA) cell-lysis buffer (150 mM NaCl, 1% Triton-X-100, 0.1% sodium dodecyl sulfate (SDS), 50 mM Tris, pH 8.0, 10 mM sodium fluoride, 1 mM sodium orthovanadate, and complete protease inhibitor cocktail (1 tablet/10 ml)). The cells were sonicated or vortexed every 10 min while kept on ice for 30 min. The cell lysate was collected after centrifuging at 14,000 × *g* for 15 min at 4 °C. The protein concentration was measured using Pierce BCA Protein Assay (Thermo Fisher Scientific, Waltham MA). The samples were prepared with Laemmli sample buffer and loaded onto (4–15%) gradient gels for SDS–PAGE (SDS–PAGE) electrophoresis. After electrophoresis, the gels were equilibrated in cold transfer buffer and transferred to polyvinylidene difluoride (PVDF) membranes overnight. The membranes were blocked with Odyssey Blocking Buffer and incubated with appropriate rabbit primary antibodies (Table 1) along with mouse

monoclonal actin antibody, which was used for normalization. After washing with PBS, 0.1% Tween-20 (4 × 5 min), the membranes were incubated with secondary antibodies (goat anti-rabbit IRDye 680RD and goat anti-mouse IRDye 800CW) for 30–60 min. The membranes were washed and scanned on an Odyssey Infrared imager (LI-COR).

Dose–response analysis of intracellular signaling in primary HRMECs: HRMECs were seeded into black 96-well plates (5,000/well) that had been coated with attachment factor. The cells were grown to confluence using fully supplemented EndoGRO-MV media for 4–5 days. The cells were serum starved overnight using EndoGRO-MV without hydrocortisone. The cells were treated with $VEGFA_{165}a$ or $VEGFA_{165}b$ for various lengths of time after which the treatments were immediately removed and replaced with 4% paraformaldehyde. They were fixed for 20 min at room temperature followed by permeabilization with PBS, 0.1% Triton X-100 (10 min). The cells were blocked by incubation with Odyssey Blocking Buffer (Li-Cor) for 1.5 h at room temperature and incubated with primary antibodies (1:200) for either 2 h at room temperature or overnight at 4 °C. Rabbit antibodies were used against the proteins of interest, and a mouse monoclonal anti-beta-actin antibody was used for normalization. The cells were washed with PBS, 0.1% Tween-20 (5 × 5 min) and incubated with secondary antibodies, goat anti-rabbit IRDye 800CW and goat anti-mouse IRDye 680RD (1:750) for 45 min at room temperature. After washing with PBS 0.1% Tween-20 (5 × 5 min), the plates were scanned on an Odyssey Imager (Li-Cor). For time–response and dose–response experiments, the doses of $VEGFA_{165}a$ and $VEGFA_{165}b$ were assayed in quadruplicate wells, and dose–response experiments were repeated three times to confirm reproducibility of relative dose–response curves for activation of MAPK (phospho-Thr202/Tyr204), AKT (phospho-Ser473), and VEGFR2 (phospho-Tyr1175). Data were fit to a four-parameter log-logistic response function Equation (1) at the 95% confidence level for each dose *x* using the Drc package for R [37]. The parameters fit were *b*, the steepness of the curve at *e* the median effective dose (ED_{50}), with *c* and *d* the lower and upper limits of the response. The 95% confidence level for fitting was used to produce curves:

$$f(x,(b,c,d,e)) = c\frac{(d-c)}{(1+\exp(b(\log(x)-\log(e)))}$$

Quantitative PCR analysis of HRMEC gene expression: Primary HRMECs were grown to confluence in six-well plates. After the desired treatment, the cells were trypsinized. Total RNA was isolated using the Absolutely RNA Miniprep kit (Agilent, Santa Clara, CA). The cells were homogenized in 20 µl of lysis buffer. Homogenization was accomplished using conical pellet pestles in 1.5 ml microfuge tubes, with a handheld rotary tool (Bel-Art, Wayne, NJ). First-strand cDNA was synthesized by reverse transcribing 500 ng of total RNA per sample using either the AffinityScript qPCR DNA Synthesis kit (Agilent) or the LunaScript RT SuperMix Kit (NEB # E3010(S/L), Ipswich, MA) with Oligo-dT priming. The reaction conditions were according to the manufacturer's instructions. For AffinityScript: 25 °C for 5 min, 42 °C for 20 min, 95 °C for 5 min, and 10 °C for 10 min. For LunaScript RT: 25 °C for 2 min, 55 °C for 10 min, and 95 °C for 1 min. All compared samples were processed using the same reagent set. Stock first-strand cDNA preparations were stored at −70 °C and were not used for analysis after a maximum of three freeze–thaws. The duplex reaction format was used with FAM-labeled probe and primer pairs for the gene of interest and VIC-labeled probe and primer-limited pairs for tata-binding protein (*TBP,* Gene ID 6908; OMIM 60075) as the normalizer gene (ThermoFisher, Waltham, MA). For real-time PCR reactions, sample first-strand cDNA was diluted fivefold with deionized water, and 2 µl added to 18 µl of Master Mix for 20 µl PCR reactions. Triplicate reactions were used for each sample. Master Mix chemistries were either 2X Gene Expression Master Mix (ThermoFisher, Applied Biosystems, Waltham, MA), or the Luna Universal Probe qPCR Master Mix (2X) Gene Expression (New England BioLabs # M3004L, Ipswich, MA), both mixes with the Rox reference dye option. Reactions were run on either an Mx3000P real-time PCR system using MxPro software or an AriaMx Real-time PCR System using the AriaMx HRM QPCR Software (Agilent). Gene expression assays were evaluated for high PCR efficiency using a dilution series of HRMEC cDNA to ensure validity of using the delta-delta Ct method for comparing relative gene expression. Each replicate reaction was internally normalized relative to endogenous *TBP* gene expression. The specific assay probe sets used for gene expression analysis are listed in Table 2.

Table 2. Taqman gene expression probes for *HRMEC* gene expression.

Gene	Probe Set #	Spans Exons
CLDN5	Hs01561351_m1	1–2
ICAM1	Hs00164932_m1	2–3
OCLN	Hs00170162_m1	5–6
SELE	Hs00174057_m1	4–5
TBP	Hs00427620_m1	3–4
VCAM1	Hs01003372_m1	6–7

RESULTS

Preliminary observations: The cell-based experimental results reported here were inspired by observations made during preliminary testing for a different project to develop an intravitreal injection model using $VEGFA_{165}$a to cause dilation of primary retinal veins, which was reported to occur in the Long Evans rat [38]. That model typically involves a high dose of VEGFA. Using fluorescein angiography, and SD-OCT imaging, it was noted that similar effects on the vasculature could be induced with $VEGFA_{165}$b or $VEGFA_{165}$a. Although the observational studies did not use large numbers of rats, they are included as supplemental observations (Appendix 1) because they brought to our attention that the dose–responses for intracellular pathway activation were not fully known in primary human retinal endothelial cells.

Activation of MAPK and AKT in primary HRMECs by $VEGFA_{165}$a and $VEGFA_{165}$b: To examine the effect of $VEGF_{165}$ isoforms on intracellular signaling pathways, we chose primary HRMECs and initially used immunoblotting to test activation of the MAPK and AKT pathways by both isoforms. These pathways were examined as two of the intracellular signaling kinases implicated in mediating the effects of VEGFA on endothelial proliferation and the blood–retinal barrier. Under a high dose (100 ng/ml, 5,300 pM) for maximum activation, both isoforms of $VEGFA_{165}$ increased the amounts of the active form of MAPK (Figure 1A) and the active form of AKT (Figure 1B). From three separate full experimental repeats, the average activation was about 2.7-fold and 1.6-fold (Figure 1C) for MAPK and AKT, respectively. Although the treatments with $VEGFA_{165}$a and $VEGFA_{165}$b always increased the activation of both kinases, the magnitude of the increase varied between experiments as illustrated by the comparison of two of the three experiments on the same gel (Figure 1A,B).

Dose–response for the activation of MAPK by $VEGFA_{165}$a and $VEGFA_{165}$b: Although repeated immunoblotting experiments confirmed activation of MAPK and AKT by both $VEGFA_{165}$ isoforms, the experimental variability introduced by protein extraction, protein assays, electrotransfer, band shape, and image analysis was judged to be unsuitable for dose–response analysis. To address the variability, new in situ assays, or ICW assays, were developed using the same kinase-specific antibodies while removing the sample processing required for immunoblotting. This also permitted faster fixation of cells at the desired time, the use of many doses, and the use of several biologic replicates per dose.

The maximum activation of the MAPK (ERK1/2) pathway in primary HRMECs occurred at 10 min for treatment with $VEGFA_{165}$a and $VEGFA_{165}$b, and returned to control levels by 90 min, using a dose of 2 ng/ml (1,050 pM). See Figure 2A. The activation of $VEFGA_{165}$a was statistically significantly stronger than that of $VEGFA_{165}$b at 10 min (*t* test, $p<0.01$).

We next performed dose–response analysis for the activation of the MAPK at 10 min with cells preadapted to lower serum. Eleven doses of each isoform, with four biologic replicates per dose, were evaluated, and the dose–response data for MAPK activation were fit to the log-logistic four-parameter dose–response function using the Drc package in R [37] (Figure 2B). Activation of MAPK by $VEGFA_{165}$b showed a typical sigmoidal dose–response. Compared to $VEGFA_{165}$b, the dose–response curve for $VEGFA_{165}$a displayed a strong allosteric shift to a binary-like activation response. $VEGFA_{165}$a was more potent for activation of MAPK at lower doses. A similar maximum level of MAPK activation could be achieved with the highest dose tested (10,000 pM) using either isoform. Activation of MAPK by $VEGFA_{165}$b was only 10% of that generated by $VEGFA_{165}$a using a dose of 250 pM. The ED_{50} was 73 pM for $VEGFA_{165}$a and 1015 pM for $VEGFA_{165}$b for the experiment shown. The experiment was repeated three times confirming the large difference in ED_{50} between the two isoforms. Differences between the ED_{50} values were typically in the 800 to 1,000 pM range.

Dose–response for the activation of AKT activation by $VEGFA_{165}$a and $VEGFA_{165}$b: Maximum activation of the AKT pathway in HRMECs occurred 30 min after treatment with $VEGFA_{165}$a and 15 min after treatment with $VEGFA_{165}$b (Figure 3A) using what was thought to be a maximum activating dose (100 ng/ml, 5,300 pM). Dose response analysis was performed for AKT activation using these respective maximum time points, and the data were fit to the four-parameter log-logistic response function (Figure 3B). With $VEGFA_{165}$a, AKT activation in HRMECs displayed a much steeper dose–response curve than for $VEGFA_{165}$b. The ED_{50} values were 53 pM for $VEGFA_{165}$a compared to 126 pM for $VEGFA_{165}$b. The maximum activation of AKT generated by the b-isoform was less than half that obtained from treatment with the a-isoform. Repetition of the experiment confirmed similar relative responses.

Dose–response for the activation of VEGFR2 by $VEGFA_{165}$a and $VEGFA_{165}$b: To test for relative differences in dose–response at the level of the receptor itself, we examined the dose–response for activation of VEGFR2. Maximum activation of the receptor was fast, within less than several minutes, as quickly as cells could be processed for treatment and fixation. The 5 and 10 min experiments were similar in relative response. Therefore, 10 min were used for the

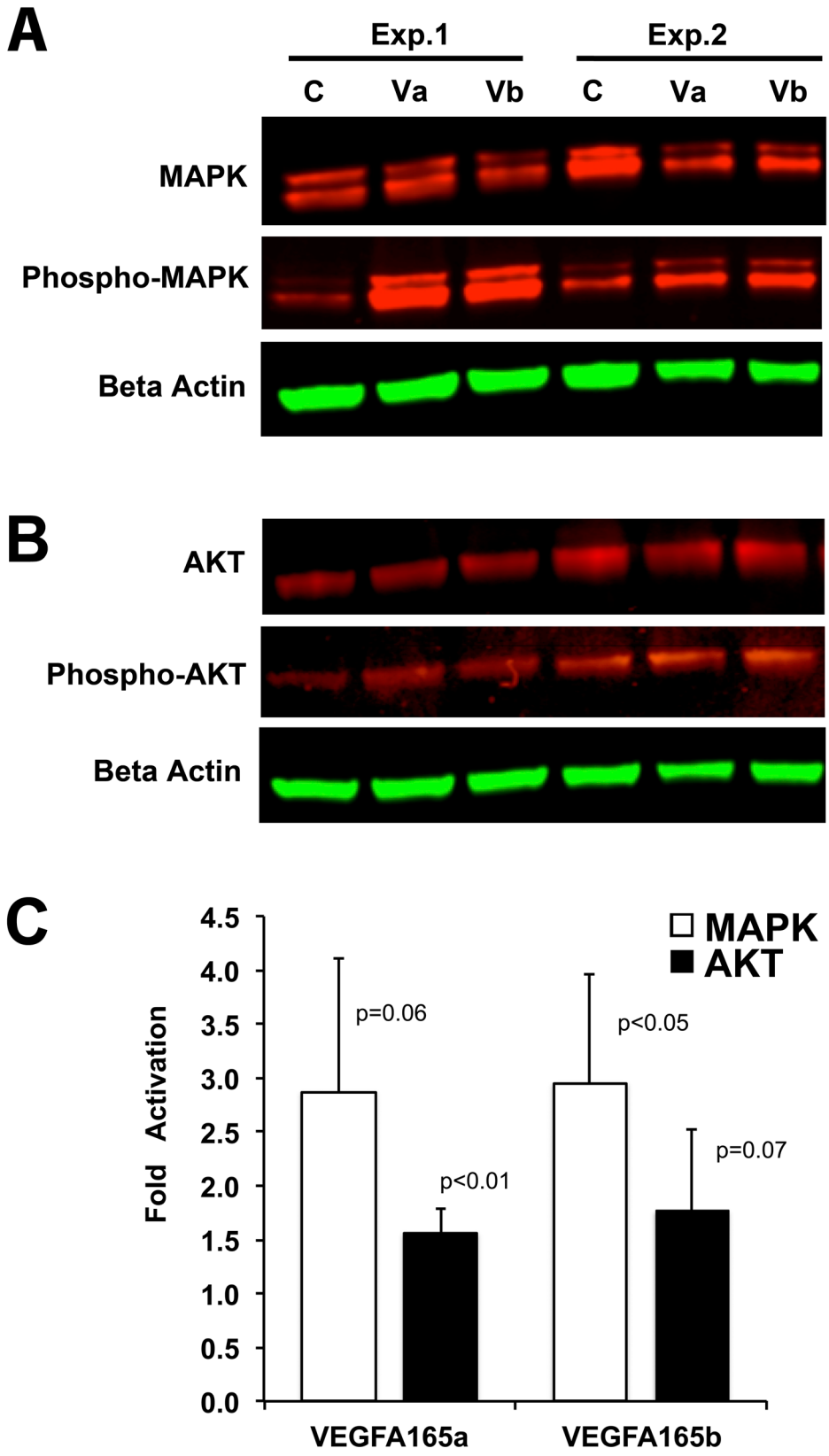

Figure 1. MAPK and AKT are activated in HRMECs by $VEGFA_{165}a$ and $VEGFA_{165}b$. **A**: Immunoblots of total MAPK and activated MAPK (phospho-MAPK) 10 min after treatment with $VEGFA_{165}a$ (Va), $VEGFA_{165}b$ (Vb), or media control (C). Two representative experiments are shown. **B**: Immunoblots of total AKT and activated AKT (phospho-AKT) 10 min after treatment with $VEGFA_{165}a$ (Va), $VEGFA_{165}b$ (Vb), or media control (C). Two representative experiments are shown. **C**: Fold activation of MAPK and AKT from three immunoblotting experiments. P values are shown, *t* test relative to media controls (onefold).

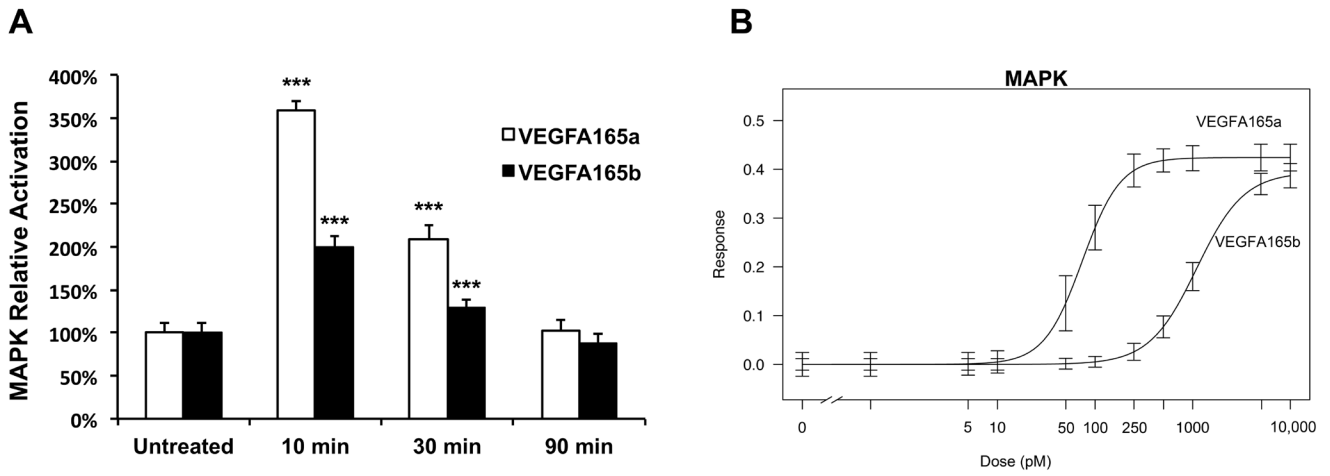

Figure 2. VEGFA$_{165}$a strongly activates MAPK in primary HRMECs at doses where VEGFA$_{165}$b has little effect. Activation of MAPK was measured with in situ immunofluorescence with a phosphospecific antibody (phospho-Thr202/Tyr204) for p44/42. **A**: Activation of MAPK at three time points after the addition of 1,000 pM VEGFA$_{165}$a or VEGFA$_{165}$b. Bar shows standard deviation. (*t* test, ***p<0.001 relative to untreated control, n=8 biologic replicates.) **B**: Dose–response curves for activation of MAPK. The median effective dose (ED$_{50}$) was 73 pM for VEGFA$_{165}$a and 1,015 pM for VEGFA$_{165}$b. Bars indicate the 95% confidence interval for data fit to the four-parameter log-logistic function. n=4 biologic replicates per dose.

dose–response experiments, and data were fit to the four-parameter log-logistic response function as shown in Figure 4. The VEGFA$_{165}$a treatment achieved maximum activation by about 500 pM, whereas VEGFA$_{165}$b caused little if any activation at that dose. The ED$_{50}$ for activation by VEGFA$_{165}$a was 254 pM compared to 1,192 pM for the VEGFA$_{165}$b. Furthermore, the maximum activation by VEGFA$_{165}$b was 73% of that obtained with VEGFA$_{165}$a. The relative pattern was confirmed with a repeated experiment (data not shown).

Isoform effects on expression leukocyte-docking protein genes: We first examined gene expression from 1 to 24 h after treatment with high doses (100 ng/ml, 5,300 pM) of

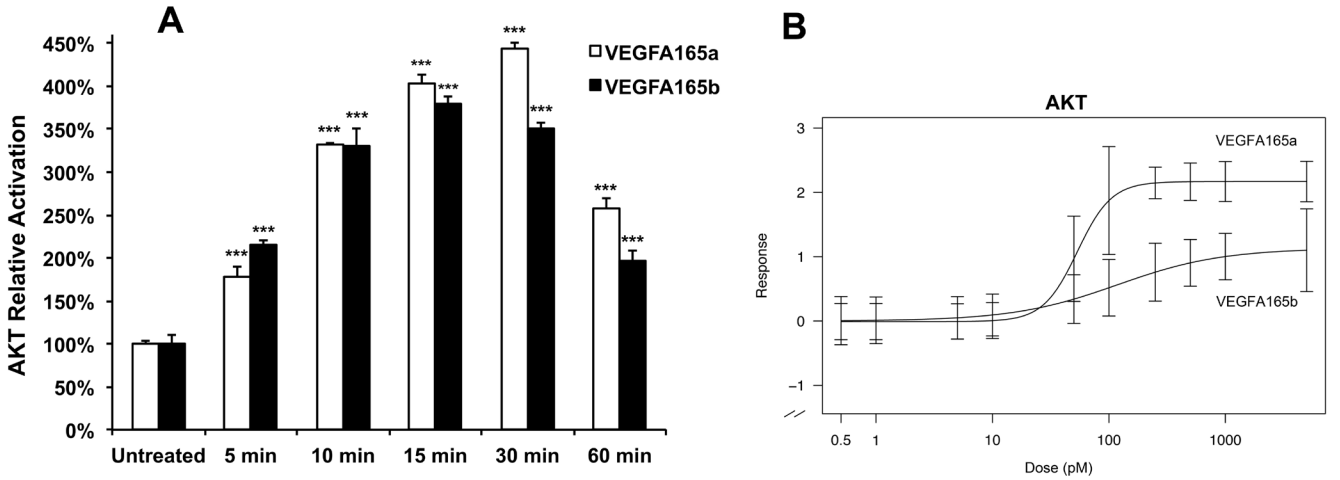

Figure 3. VEGFA$_{165}$b is a weaker activator of AKT in primary HRMECs compared to VEGFA$_{165}$a. **A**: Activation of AKT was measured with in situ immunofluorescence with a phosphospecific antibody for Ser473-AKT at five time points after the addition of 20 ng/ml (1,050 pM) VEGFA$_{165}$a or VEGFA$_{165}$b. Bar shows standard deviation. (*t* test, ***p<0.001 relative to untreated control, n=4 biologic replicates.) **B**: Dose–response curves for activation of AKT. The median effective dose (ED$_{50}$) value for AKT activation by VEGFA$_{165}$a was 53 pM compared to 126 pM for VEGFA$_{165}$b. Bars indicate the 95% confidence interval for data fit to the four-parameter log-logistic function. n=4 biologic replicates per dose.

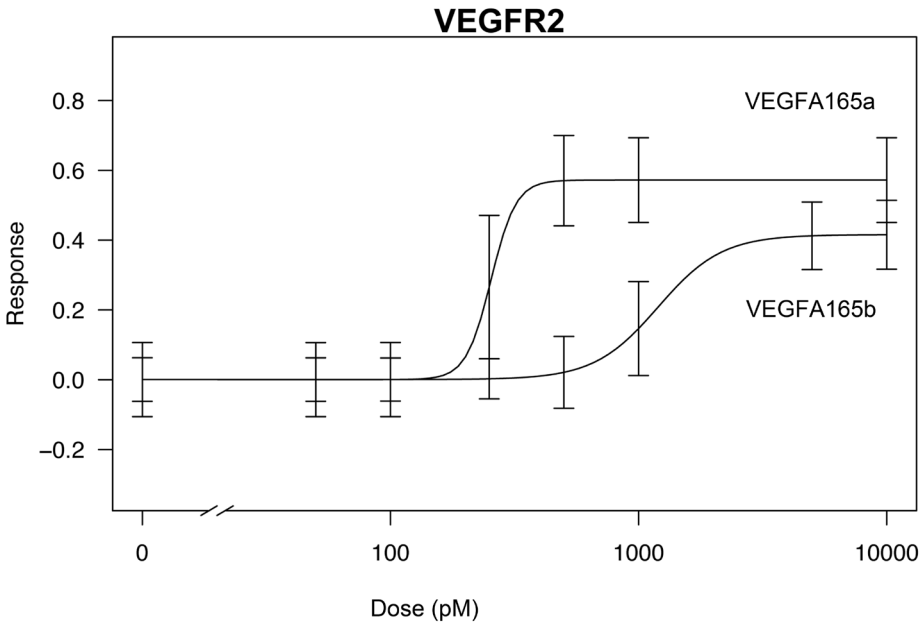

Figure 4. Differences in the activation of intracellular signaling between VEGFA$_{165}$a and VEGFA$_{165}$b in primary HRMECs begin at the receptor VEGFR2. VEGFA$_{165}$a was a stronger activator of VEGFR2 compared to VEGFA$_{165}$b. The median effective dose (ED$_{50}$) for activation by VEGFA$_{165}$a was 254 pM compared to 1,192 pM for VEGFA$_{165}$b. Bars indicate the 95% confidence interval for data fit to the four-parameter log-logistic function. n=4 biologic replicates per dose.

VEGFA$_{165}$a and VEGFA$_{165}$b to determine the optimal time point for monitoring any effects on the expression of *ICAM1* (Gene ID 3383; OMIM 147840), *SELE* (Gene ID 6401; OMIM 131210), *VACAM1* (Gene ID 7412; OMIM 192225). A dose of 5,300 pM was likely a saturating concentration and more than what would be experienced in vivo, to find a suitable time point when gene expression could be subsequently compared using physiologically relevant doses. All three of these genes displayed increased expression after treatment with both isoforms of VEGFA$_{165}$ (Figure 5A,C,E). These trends were confirmed with repeated experiments (data not shown). Of the genes examined, the increasing expression trend of *ICAM1* was more variable in timing, not always maximum at 6 h, sometimes later by 24 h (data not shown).

Selecting a fixed treatment time of 6 h, and guided by the activation dose–response curves for MAPK and AKT, we tested low (2 ng/ml, 100 pM), intermediate (19 ng/ml, 1,000 pM), and high (95 ng/ml, 5000 pM) doses to test for differences in the effects on leukocyte-docking gene expression. For all three leukocyte-docking protein genes (*ICAM1, SELE,* and *VCAM1*), VEGFA$_{165}$a increased their expression at the intermediate dose of 1,000 pM, where VEGFA$_{165}$b still had very little effect (Figure 5D,F,G).

Isoform effects on expression of tight junction protein genes: The effects of VEGFA$_{165}$a and VEGFA$_{165}$b on the expression of the two key tight junction protein genes, *CLDN5* (Gene ID 7122; OMIM 608102), *OCLN* (Gene ID 100,506,658; OMIM 602876), were also compared. These genes encode the tight junction proteins CLDN5 and OCLN; see Figure 6. Both isoforms of VEGFA$_{165}$ reduced the expression of these genes by the 6-h time point (Figure 6A,C). We next compared low (2 ng/ml, 100 pM), intermediate (19 ng/ml, 1,000 pM), and high saturating doses (95 ng/ml, 5,000 pM) at the fixed 6 h time point. VEGFA$_{165}$b was less effective at suppressing the expression of *CLDN5* and *OCLN* compared to VEGFA$_{165}$a (Figure 6D,F).

DISCUSSION

Although the role of VEGFA in vascular development, tumorgenesis, and hypoxia has been investigated for almost three decades, less is known about the functional differences between VEGFA isoforms. Recently, isoform-specific analysis reported that most VEGFA$_{165}$ in normal vitreous was VEGFA$_{165}$b, with the ratio changing to mostly VEGFA$_{165}$a in eyes with active diabetic retinopathy and ROP [33,34]. The relative expression of VEGFA$_{165}$a and VEGFA$_{165}$b can be regulated by alternative splicing of the VEGFA$_{165}$ pre-mRNA, which is regulated by phosphorylation of the ASF/SF2 splicing factor by SR-protein kinase (SRPK1/2) [39]. This raised the possibility that modulation of this isoform ratio might be exploited for therapeutic purposes. Modulation of the splicing between the VEGFA$_{165}$a and VEGFA$_{165}$b mRNAs

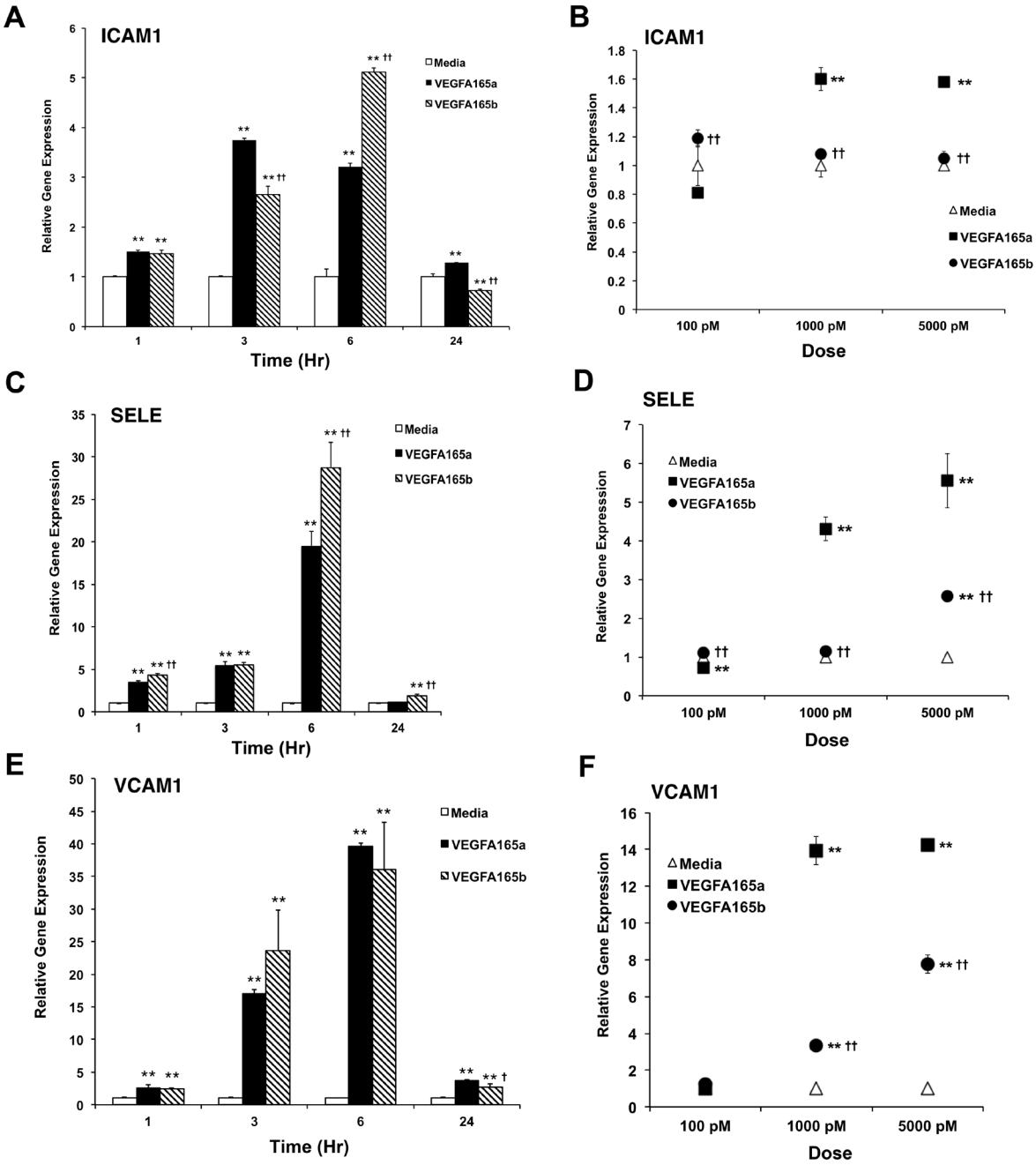

Figure 5. $VEGFA_{165}a$ has a stronger effect on leukocyte–endothelial cell adhesion gene expression in primary HRMECs than $VEGFA_{165}b$. Relative gene expression was measured with quantitative PCR (qPCR). **A**: Expression of the *ICAM1* gene at 1, 3, 6, and 24 h after treatment with $VEGFA_{165}$. Confluent human retinal microvascular endothelial cells (HRMECs) were treated with a saturating high dose of $VEGFA_{165}a$ or $VEGFA_{165}b$ (100 ng/ml, 5,300 pM). **B**: Expression of the *ICAM1* gene comparing $VEGFA_{165}a$ and $VEGFA_{165}b$ at low, intermediate, and high doses measured after 6 h. **C**: Expression of the *SELE* gene at 1, 3, 6, and 24 h after treatment with $VEGFA_{165}$. **D**: Expression of the *SELE* gene comparing $VEGFA_{165}a$ and $VEGFA_{165}b$ at low, intermediate, and high doses measured after 6 h. **E**: Expression of the *VCAM1* gene at 1, 3, 6, and 24 h after treatment with $VEGFA_{165}$. **F**: Expression of the *VCAM1* gene comparing $VEGFA_{165}a$ and $VEGFA_{165}b$ at low, intermediate, and high doses measured after 6 h. (Triplicate assays, error bars show standard deviation. ANOVA (ANOVA): compared to media control *p<0.05, **p<0.01; compared to $VEGFA_{165}a$ †p<0.05, ††p<0.01).

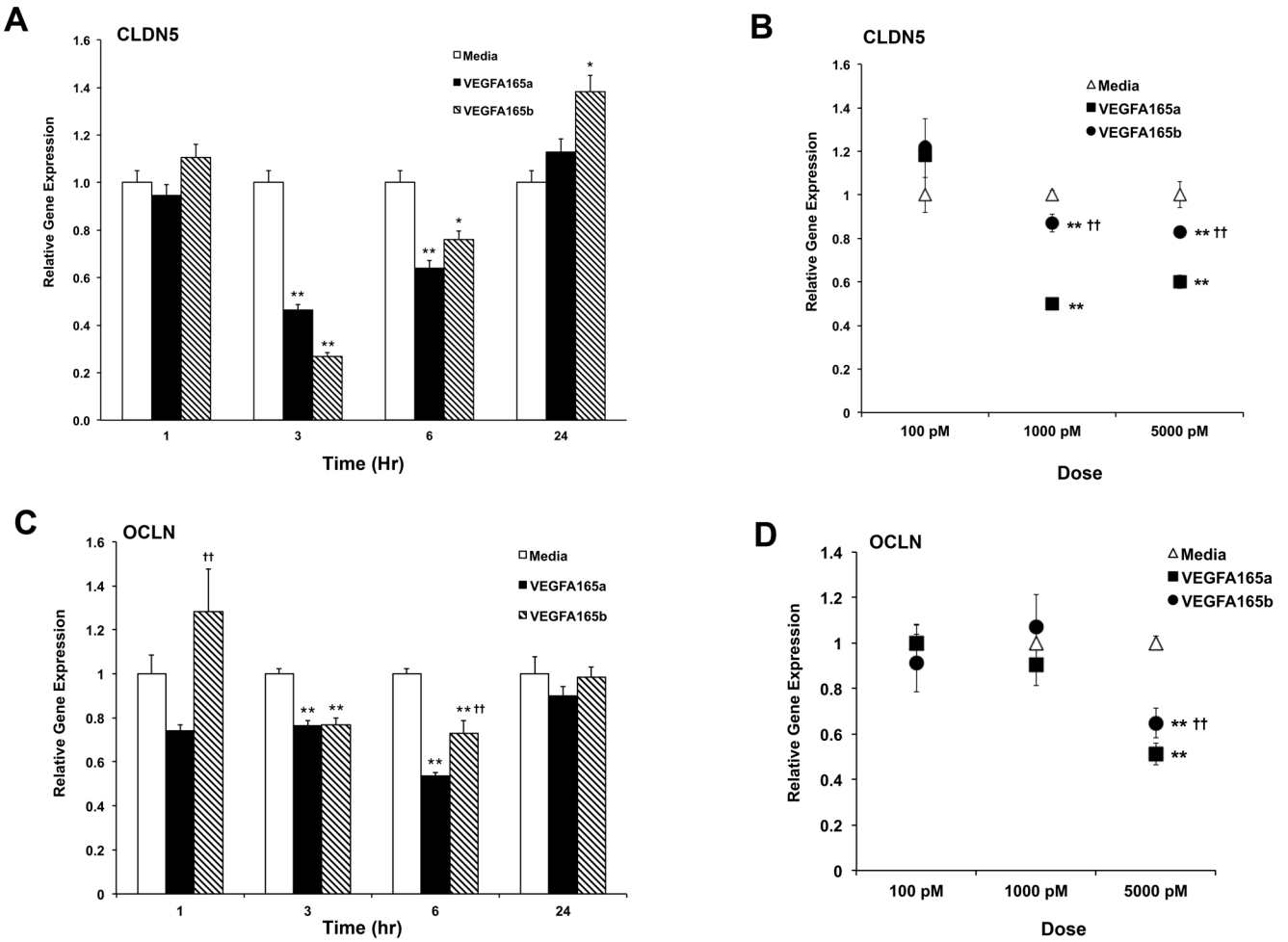

Figure 6. $VEGFA_{165}a$ has a stronger effect on the expression of tight-junction-protein genes in primary HRMECs than $VEGFA_{165}b$. Relative gene expression measured with quantitative PCR (qPCR). **A**: Expression of the *CLDN5* gene at 1, 3, 6, and 24 h after treatment with $VEGFA_{165}$. Confluent human retinal microvascular endothelial cells (HRMECs) were treated with a saturating high dose of $VEGFA_{165}a$ or $VEGFA_{165}b$ (100 ng/ml, 5,300 pM). **B**: Expression of the *CLDN5* gene comparing $VEGFA_{165}a$ and $VEGFA_{165}b$ at low, intermediate, and high doses measured after 6 h. **C**: Expression of the *OCLN* gene at 1, 3, 6, and 24 h after treatment with $VEGFA_{165}$. **D**: Expression of the *OCLN* gene comparing $VEGFA_{165}a$ and $VEGFA_{165}b$ at low, intermediate, and high doses measured after 6 h. (Triplicate assays, error bars show standard deviation. ANOVA (ANOVA): compared to media control *p<0.05, **p<0.01; compared to $VEGFA_{165}a$ †† p<0.01).

was demonstrated using SRPK inhibitors in human RPE cells, and topical infusion of these inhibitors reduced neovascularization in a mouse laser-induced choroidal neovascularization (CNV) model [40]. Another group used intravitreal injection of a different SRPK inhibitor to inhibit neovascularization in the mouse CNV model [41]. An antibody specific for the C-terminus of $VEGFA_{165}a$, which does not bind $VEGFA_{165}b$, can also inhibit the proangiogenic effects of $VEGFA_{165}a$ [42].

Specific blockade of the $VEGFA_{165}a$ protein, or suppressing $VEGFA_{165}a$ expression in favor of $VEGFA_{165}b$, could be a therapeutic strategy if there are significant differences in the ability of these isoforms to activate intracellular signaling in the retinal endothelium. The preference for examining signaling differences using primary HRMECs is supported by studies that revealed differences between endothelial cells derived from different organs. For example, viral delivery of murine recombinant-$VEGF_{164}b$ attenuated inflammatory-response damage in a murine model of ulcerative colitis, yet it exacerbated damage in the blood–brain barrier in a model of focal cerebral ischemia [43-45]. Extensive gene expression profiling has also demonstrated that HUVECs have greater expression of embryonic genes, and other differences, compared to endothelial cells from the choroid and neural retina. Significant differences also exist between human retinal endothelial cells and human choroidal

endothelial cells in the expression of genes that are related to endothelial function and neovascularization [46].

We began with immunoblotting to examine the activation of MAPK and AKT in primary HRMECs. Although $VEGFA_{165}b$ does not bind the neuropilin 1 coreceptor, it does bind to VEGFR2 with similar or less affinity as $VEGFA_{165}a$ depending on the cell model and method used [31,32]. Regardless of relative binding affinity, $VEGFA_{165}b$ is reported to bind and activate VEGFR2 based on immunoblotting studies [31,47,48]. Using immunoblotting, we found that MAPK and AKT were activated to a similar extent by $VEGFA_{165}a$ or $VEGFA_{165}b$, using a dose of 100 ng/ml (5,300 pM) in primary HRMECs. Previous single-dose immunoblotting studies in different cell types reported that $VEGFA_{165}b$ activated VEGFR2 and MAPK less than $VEGFA_{165}a$, and that the maximum activation of MAPK by $VEGFA_{165}b$ occurred later than $VEGFA_{165}a$ in PAE cells and bovine aortic endothelial cells using a dose of 2,600 pM [31,47]. Another study of human pulmonary microvascular endothelial cells (HPMECs) found that the a-isoform was a stronger activator of VEGFR2 and MAPK (ERK1/2) than the b-isoform at a dose of 20 ng/ml (1,050 pM) [48].

We found that MAPK and AKT were activated less by $VEGFA_{165}b$ at the lower dose (20 ng/ml, 1,000 pM; data not shown). However, it was noted that although activation was detected in repeated experiments, the relative magnitude of activation was variable using immunoblotting. Immunoblotting involves numerous processing steps, and a substantial number of cells are required for a single sample; therefore, we decided that in situ assays would be superior for generating full dose–response curve data.

To determine the dose–response for activation of MAPK and AKT, in situ ICW assays were developed that permitted the use of multiple replicate doses with a limited supply of primary cells in a 96-well plate format. The resulting dose–response curves confirmed that there were substantial differences in the activation of MAPK and AKT between $VEGFA_{165}a$ and $VEGFA_{165}b$ in primary HRMECs. In the case of MAPK, the ED_{50} of $VEGFA_{165}a$ was 900 pM less than the ED_{50} for $VEGFA_{165}b$. $VEGFA_{165}a$ caused near maximum activation of MAPK at a concentration of 250 pM, while $VEGFA_{165}b$ had little effect at 250 pM. Higher doses of $VEGFA_{165}b$ could activate MAPK to a similar maximum level, and the timing for maximum activation of MAPK was similar for both isoforms in HRMECs, occurring by 10 min and decreasing by 30 min. This relative timing was different from that reported for HUVECs where the maximum concentration of active MAPK occurred 30 min after treatment with $VEGFA_{165}b$ [31].

For AKT, the difference in ED_{50} between $VEGFA_{165}a$ and $VEGFA_{165}b$ was not as large as seen for MAPK, just twofold greater for $VEGFA_{165}b$ compared to $VEGFA_{165}a$. However, the activation of AKT by $VEGFA_{165}b$ was substantially less than from $VEGFA_{165}a$ over the entire dose–response range. In contrast to MAPK activation, the time to maximum activation of AKT was earlier with $VEGFA_{165}b$ (15 min) compared to the $VEGFA_{165}a$ (30 min). Although the differences in the ED_{50} values were not as large as seen for MAPK activation, the maximum activation of AKT obtained with $VEGFA_{165}b$ was only 50% of the maximum activation generated by $VEGFA_{165}a$. This was another difference from that reported in a non-retinal endothelial cell type, human pulmonary endothelial cells (HPECs), where AKT activation is the same for $VEGFA_{165}a$ and $VEGFA_{165}b$ at a dose of 20 ng/ml (1,050 pM) in HPECs [48].

The differences noted above in the activation of MAPK and AKT between HRMECs and non-retinal endothelial cells suggest that VEGF-mediated intracellular signaling patterns are not completely universal between endothelial cells from different organs. An evaluation of primary endothelial cells from the human retina should be used whenever possible to study the retinal context. Altogether the dose–response curves for the activation of VEGFR2, MAPK, and AKT in primary HRMECs were consistent with the model proposed by Whitaker et al., in which $VEGFA_{165}a$ activates VEGFR2 more intensely when it can bind the coreceptor neuropilin 1, to form a larger activation complex [49].

Based on the primary HRMEC dose–response data for MAPK activation, $VEGFA_{165}a$ was more potent for activating intracellular signaling than $VEGFA_{165}b$ at lower doses, which fall into a range of total $VEGFA_{165}a$ concentrations previously reported in human vitreous. Vitreous concentrations for VEGFA have been measured with various techniques in several disease conditions. The most elevated VEGFA is the $VEGFA_{165}$ isoform, which diffuses slowly, and the vitreous has protease activity; therefore, it is possible that the concentrations measured in the vitreous are somewhat lower than in the neural retina itself. With that stated, vitreal concentrations of 25 pM to more than 400 pM have been reported for proliferative diabetic retinopathy by several studies [1,50-54]. Other studies have reported 10 pM in diabetic macular edema [55], 100 to 450 pM in retinopathy of prematurity [34,56] and an average of 430 pM, with as high as 580 pM, in central retinal vein occlusion [57]. It is possible that elevations of retinal $VEGFA_{165}a$ concentration to several hundred picomolars could increase the activation of endothelial intracellular signaling above its normal baseline. In contrast, the much lower activation potential of $VEGFA_{165}b$ in this concentration

range would leave MAPK activation close to normal if most of the VEGFA$_{165}$ existed as the b-isoform.

We also found that VEGFA$_{165}$b could affect the expression of the same target genes that are also regulated by VEGFA$_{165}$a in primary HRMECs. These included genes involved in leukocyte–endothelial cell adhesion and the formation of tight junctions. Although the 5,000 pM dose of VEGFA$_{165}$b could activate MAPK and AKT more strongly than the intermediate 1,000 pM dose, it is unlikely that the 5,000 pM concentration would be experienced in vivo. For that reason, we suggest that the effects on gene expression at 1,000 pM were most informative. We found that the *CLDN5* gene was particularly susceptible to repression by both isoforms of VEGFA$_{165}$ compared to *OCLN* in this cell type. VEGFA-mediated activation of the VEGFR2 receptor is known to disrupt adherin junctions and causes β-catenin-mediated repression of the expression of the *CLDN5* gene in endothelial cells [58]. For all three leukocyte-docking protein genes (*ICAM1, SELE, VCAM1*), VEGFA$_{165}$a increased their expression at the intermediate dose of 1,000 pM, where VEGFA$_{165}$b had less effect. We concluded that there were substantial dose–response differences in the regulation of VEGFA target genes, with VEGFA$_{165}$a proving to be the stronger effector of gene expression overall.

Conclusion: The results indicated that differences in the last six amino acids between VEGFA$_{165}$a and VEGFA$_{165}$b have a significant effect on the relative activation of MAPK and AKT within primary HRMECs. VEGFA$_{165}$a activated both pathways at lower concentrations where VEGF$_{165}$b had little effect. The greater potential of VEGFA$_{165}$a to affect HRMECs also extended to changes in the expression of genes required for leukocyte-docking and tight-junction structure. Large dose–response differences in activation of these pathways exist in ranges of elevated VEGFA$_{165}$a concentrations that have been reported in the vitreous of diseased eyes. Key aspects of MAPK and AKT activation, such as timing and maximum activation, were different in HRMECs compared to those reported for some other non-retinal endothelial cell types. These results would support the concept that specific blockade of VEGFA$_{165}$a, or modulating the VEGFA$_{165}$b/VEGFA$_{165}$a ratio, could be useful therapeutic strategies for retinal diseases involving elevated VEGFA concentrations.

APPENDIX 1. SUPPLEMENTAL OBSERVATIONS

To access the data, click or select the words "Appendix 1." Supplemental observations file of observations data for readers to download.

ACKNOWLEDGMENTS

The authors thank Oakland University students Regan Miller and Anju Thomas for assistance with some cell culture and some testing of gene expression probesets used for these studies. Research supported by National Eye Institute / National Institutes of Health (USA) grant NIH R15EY025089 (KPM).

REFERENCES

1. Aiello LP, Avery RL, Arrigg PG, Keyt BA, Jampel HD, Shah ST, Pasquale LR, Thieme H, Iwamoto MA, Park JE. Vascular endothelial growth factor in ocular fluid of patients with diabetic retinopathy and other retinal disorders. N Engl J Med 1994; 331:1480-7. [PMID: 7526212].

2. Miller JW, Adamis AP, Aiello LP. Vascular endothelial growth factor in ocular neovascularization and proliferative diabetic retinopathy. Diabetes Metab Rev 1997; 13:37-50. [PMID: 9134347].

3. Robbins SG, Conaway JR, Ford BL, Roberto KA, Penn JS. Detection of vascular endothelial growth factor (VEGF) protein in vascular and non-vascular cells of the normal and oxygen-injured rat retina. Growth Factors 1997; 14:229-41. [PMID: 9386988].

4. Amadio M, Govoni S, Pascale A. Targeting VEGF in eye neovascularization: What's new?: A comprehensive review on current therapies and oligonucleotide-based interventions under development. Pharmacol Res 2016; 103:253-69. [PMID: 26678602].

5. Avery RL, Castellarin AA, Steinle NC, Dhoot DS, Pieramici DJ, See R, Couvillion S, Nasir MA, Rabena MD, Le K, Maia M, Visich JE. Systemic pharmacokinetics following intravitreal injections of ranibizumab, bevacizumab or aflibercept in patients with neovascular amd. Br J Ophthalmol 2014; 98:1636-41. [PMID: 25001321].

6. Li Y-L, Zhao H, Ren X-B. Relationship of VEGF/VEGFR with immune and cancer cells: staggering or forward? Cancer Biol Med 2016; 13:206-14. [PMID: 27458528].

7. Quinn TP, Peters KG, De Vries C, Ferrara N, Williams LT. Fetal liver kinase 1 is a receptor for vascular endothelial growth factor and is selectively expressed in vascular endothelium. Proc Natl Acad Sci USA 1993; 90:7533-7. [PMID: 8356051].

8. Millauer B, Wizigmann-Voos S, Schnürch H, Martinez R, Møller NP, Risau W, Ullrich A. High affinity VEGF binding and developmental expression suggest Flk-1 as a major regulator of vasculogenesis and angiogenesis. Cell 1993; 72:835-46. [PMID: 7681362].

9. Oelrichs RB, Reid HH, Bernard O, Ziemiecki A, Wilks AF. NYK/FLK-1: a putative receptor protein tyrosine kinase isolated from E10 embryonic neuroepithelium is expressed in endothelial cells of the developing embryo. Oncogene 1993; 8:11-8. [PMID: 8423988].

10. Park JE, Keller GA, Ferrara N. The vascular endothelial growth factor (VEGF) isoforms: differential deposition into the subepithelial extracellular matrix and bioactivity of extracellular matrix-bound VEGF. Mol Biol Cell 1993; 4:1317-26. [PMID: 8167412].

11. Ferrara N. Binding to the Extracellular Matrix and Proteolytic Processing: Two Key Mechanisms Regulating Vascular Endothelial Growth Factor Action. Mol Biol Cell 2010; 21:687-90. [PMID: 20185770].

12. Bates DO, Cui TG, Doughty JM, Winkler M, Sugiono M, Shields JD, Peat D, Gillatt D, Harper SJ. VEGF165b, an inhibitory splice variant of vascular endothelial growth factor, is down-regulated in renal cell carcinoma. Cancer Res 2002; 62:4123-31. [PMID: 12124351].

13. Qiu Y, Hoareau-Aveilla C, Oltean S, Harper SJ, Bates DO. The anti-angiogenic isoforms of VEGF in health and disease. Biochem Soc Trans 2009; 37:1207-13. [PMID: 19909248].

14. Koch S, Claesson-Welsh L. Signal transduction by vascular endothelial growth factor receptors. Cold Spring Harb Perspect Med 2012; 12:a006502-[PMID: 22762016].

15. Im E, Kazlauskas A. Regulating angiogenesis at the level of PtdIns-4,5–P2. EMBO J 2006; 25:2075-82. [PMID: 16628216].

16. Gerber HP, McMurtrey A, Kowalski J, Yan M, Keyt BA, Dixit V, Ferrara N. Vascular endothelial growth factor regulates endothelial cell survival through the phosphatidylinositol 3′-kinase/Akt signal transduction pathway. Requirement for Flk-1/KDR activation. J Biol Chem 1998; 273:30336-43. [PMID: 9804796].

17. Adini I. RhoB controls Akt trafficking and stage-specific survival of endothelial cells during vascular development. Genes Dev 2003; 17:2721-32. [PMID: 14597666].

18. Gille H, Kowalski J, Yu L, Chen H, Pisabarro MT, Davis-Smyth T, Ferrara N. A repressor sequence in the juxtamembrane domain of Flt-1 (VEGFR-1) constitutively inhibits vascular endothelial growth factor-dependent phosphatidylinositol 3′-kinase activation and endothelial cell migration. EMBO J 2000; 19:4064-73. [PMID: 10921887].

19. Takahashi T, Yamaguchi S, Chida K, Shibuya M. A single autophosphorylation site on KDR/Flk-1 is essential for VEGF-A-dependent activation of PLC-γ and DNA synthesis in vascular endothelial cells. EMBO J 2001; 20:2768-78. [PMID: 11387210].

20. Takahashi T, Ueno H, Shibuya M. VEGF activates protein kinase C-dependent, but Ras-independent Raf-MEK-MAP kinase pathway for DNA synthesis in primary endothelial cells. Oncogene 1999; 18:2221-30. [PMID: 10327068].

21. Ruan G-X, Kazlauskas A. Axl is essential for VEGF-A-dependent activation of PI3K/Akt. EMBO J 2012; 31:1692-703. [PMID: 22327215].

22. Cantley LC. The phosphoinositide 3-kinase pathway. Science 2002; 296:1655-7. [PMID: 12040186].

23. Cardone MH, Roy N, Stennicke HR, Salvesen GS, Franke TF, Stanbridge E, Frisch S, Reed JC. Regulation of cell death protease caspase-9 by phosphorylation. Science 1998; 282:1318-21. [PMID: 9812896].

24. Fulton D, Gratton JP, McCabe TJ, Fontana J, Fujio Y, Walsh K, Franke TF, Papapetropoulos A, Sessa WC. Regulation of endothelium-derived nitric oxide production by the protein kinase Akt. Nature 1999; 399:597-601. [PMID: 10376602].

25. Woolard J, Wang WY, Bevan HS, Qiu Y, Morbidelli L, Pritchard-Jones RO, Cui TG, Sugiono M, Waine E, Perrin R, Foster R, Digby-Bell J, Shields JD, Whittles CE, Mushens RE, Gillatt DA, Ziche M, Harper SJ, Bates DO. VEGF165b, an inhibitory vascular endothelial growth factor splice variant: mechanism of action, in vivo effect on angiogenesis and endogenous protein expression. Cancer Res 2004; 64:7822-35. [PMID: 15520188].

26. Soker S, Takashima S, Miao HQ, Neufeld G, Klagsbrun M. Neuropilin-1 is expressed by endothelial and tumor cells as an isoform- specific receptor for vascular endothelial growth factor. Cell 1998; 92:735-45. [PMID: 9529250].

27. Prahst C, Heroult M, Lanahan AA, Uziel N, Kessler O, Shraga-Heled N, Simons M, Neufeld G, Augustin HG. Neuropilin-1-VEGFR-2 complexing requires the PDZ-binding domain of neuropilin-1. J Biol Chem 2008; 283:25110-4. [PMID: 18628209].

28. Magnussen AL, Rennel ES, Hua J, Bevan HS, Beazley Long N, Lehrling C, Gammons M, Floege J, Harper SJ, Agostini HT, Bates DO, Churchill AJ, Long NB, Lehrling C, Gammons M, Floege J, Harper SJ, Agostini HT, Bates DO, Churchill AJ. VEGF-A165b is cytoprotective and antiangiogenic in the retina. Invest Ophthalmol Vis Sci 2010; 51:4273-81. [PMID: 20237249].

29. Konopatskaya O, Churchill AJ, Harper SJ, Bates DO, Gardiner TA. VEGF165b, an endogenous C-terminal splice variant of VEGF, inhibits retinal neovascularization in mice. Mol Vis 2006; 12:626-32. [PMID: 16735996].

30. Cébe Suarez S, Pieren M, Cariolato L, Arn S, Hoffmann U, Bogucki A, Manlius C, Wood J, Ballmer-Hofer K. A VEGF-A splice variant defective for heparan sulfate and neuropilin-1 binding shows attenuated signaling through VEGFR-2. Cell Mol Life Sci 2006; 63:2067-77. [PMID: 16909199].

31. Peach CJ, Kilpatrick LE, Woolard J, Hill SJ. Comparison of the ligand-binding properties of fluorescent VEGF-A isoforms to VEGF receptor 2 in living cells and membrane preparations using NanoBRET. Br J Pharmacol 2019; 176:3220-3235. [PMID: 31162634].

32. Perrin RM, Konopatskaya O, Qiu Y, Harper S, Bates DO, Churchill AJ. Diabetic retinopathy is associated with a switch in splicing from anti- to pro-angiogenic isoforms of vascular endothelial growth factor. Diabetologia 2005; 48:2422-7. [PMID: 16193288].

33. Zhao M, Xie WK, Bai YJ, Huang LZ, Wang B, Liang JH, Yin H, Li XX, Shi X. Expression of total vascular endothelial growth factor and the anti-angiogenic VEGF165b isoform in the vitreous of patients with retinopathy of prematurity. Chin Med J (Engl) 2015; 128:2505-9. [PMID: 26365970].

34. Zhao M, Shi X, Liang J, Miao Y, Xie W, Zhang Y, Li X. Expression of pro- and anti-angiogenic isoforms of VEGF in the mouse model of oxygen-induced retinopathy. Exp Eye Res 2011; 93:921-6. [PMID: 22067127].

35. Lomet D, Piégu B, Wood SH, Dardente H. Anti-angiogenic VEGFAxxxb transcripts are not expressed in the medio-basal hypothalamus of the seasonal sheep. PLoS One 2018; 13:e0197123-[PMID: 29746548].

36. Ritz C, Baty F, Streibig JC, Gerhard D. Dose-Response Analysis Using R. PLoS One 2015; 10:e0146021-[PMID: 26717316].

37. Miyamoto K, Khosrof S, Bursell SE, Moromizato Y, Aiello LP, Ogura Y, Adamis AP. Vascular endothelial growth factor (VEGF)-induced retinal vascular permeability is mediated by intercellular adhesion molecule-1 (ICAM-1). Am J Pathol 2000; 156:1733-9. [PMID: 10793084].

38. Nowak DG, Amin EM, Rennel ES, Hoareau-Aveilla C, Gammons M, Damodoran G, Hagiwara M, Harper SJ, Woolard J, Ladomery MR, Bates DO. Regulation of vascular endothelial growth factor (VEGF) splicing from pro-angiogenic to anti-angiogenic isoforms: a novel therapeutic strategy for angiogenesis. J Biol Chem 2010; 285:5532-40. [PMID: 19906640].

39. Gammons MV, Fedorov O, Ivison D, Du C, Clark T, Hopkins C, Hagiwara M, Dick AD, Cox R, Harper SJ, Hancox JC, Knapp S, Bates DO. Topical antiangiogenic SRPK1 inhibitors reduce choroidal neovascularization in rodent models of exudative AMD. Invest Ophthalmol Vis Sci 2013; 54:6052-62. [PMID: 23887803].

40. Hatcher JM, Wu G, Zeng C, Zhu J, Meng F, Patel S, Wang W, Ficarro SB, Leggett AL, Powell CE, Marto JA, Zhang K, Ki Ngo JC, Fu X-D, Zhang T, Gray NS. SRPKIN-1: A Covalent SRPK1/2 Inhibitor that Potently Converts VEGF from Pro-angiogenic to Anti-angiogenic Isoform. Cell Chem Biol 2018; 25:460-470.e6. [PMID: 29478907].

41. Carter JG, Gammons MVR, Damodaran G, Churchill AJ, Harper SJ, Bates DO. The carboxyl terminus of VEGF-A is a potential target for anti-angiogenic therapy. Angiogenesis 2015; 18:23-30. [PMID: 25274272].

42. Cromer W, Jennings MH, Odaka Y, Michael Mathis J, Steven Alexander J. Murine rVEGF164b, an inhibitory vegf reduces vegf-a dependent endothelial proliferation and barrier dysfunction. Microcirculation 2010; 17:536--547. .[PMID: 21040119].

43. Cromer WE, Ganta CV, Patel M, Traylor J, Kevil CG, Alexander J, Mathis J. VEGF-A isoform modulation in an preclinical TNBS model of ulcerative colitis: protective effects of a VEGF164b therapy. J Transl Med 2013; 11:207-[PMID: 24020796].

44. Chaitanya GV, Cromer WE, Parker CP, Couraud PO, Romero IA, Weksler B, Mathis JM, Minagar A, Alexander JS. A Recombinant Inhibitory Isoform of Vascular Endothelial Growth Factor164/165 Aggravates Ischemic Brain Damage in a Mouse Model of Focal Cerebral Ischemia. Am J Pathol 2013; 183:1010-24. [PMID: 23906811].

45. Browning AC, Halligan EP, Stewart EA, Swan DC, Dove R, Samaranayake GJ, Amoaku WM. Comparative gene expression profiling of human umbilical vein endothelial cells and ocular vascular endothelial cells. Br J Ophthalmol 2012; 96:128-32. [PMID: 22028475].

46. Kawamura H, Li X, Harper SJ, Bates DO, Claesson-Welsh L. Vascular endothelial growth factor (VEGF)-A165b is a weak in vitro agonist for VEGF receptor-2 due to lack of coreceptor binding and deficient regulation of kinase activity. Cancer Res 2008; 68:4683-92. [PMID: 18559514].

47. Ourradi K, Blythe T, Jarrett C, Barratt SL, Welsh GI, Millar AB. VEGF isoforms have differential effects on permeability of human pulmonary microvascular endothelial cells. Respir Res 2017; 18:116-[PMID: 28578669].

48. Whitaker GB, Limberg BJ, Rosenbaum JS. Vascular Endothelial Growth Factor Receptor-2 and Neuropilin-1 Form a Receptor Complex that is Responsible for the Differential Signaling Potency of VEGF165 and VEGF121. J Biol Chem 2001; 276:25520-31. [PMID: 11333271].

49. Li B, Li M-D, Ye J-J, Chen Z, Guo Z-J, Di Y. Vascular endothelial growth factor concentration in vitreous humor of patients with severe proliferative diabetic retinopathy after intravitreal injection of conbercept as an adjunctive therapy for vitrectomy. Chin Med J (Engl) 2020; 133:664-9. [PMID: 32068603].

50. Rezzola S, Nawaz MI, Cancarini A, Semeraro F, Presta M. Vascular Endothelial Growth Factor in the Vitreous of Proliferative Diabetic Retinopathy Patients: Chasing a Hiding Prey? Diabetes Care 2019; 42:e105-6. [PMID: 31221704].

51. Wang J, Chen S, Jiang F, You C, Mao C, Yu J, Han J, Zhang Z, Yan H. Vitreous and plasma VEGF levels as predictive factors in the progression of proliferative diabetic retinopathy after vitrectomy. PLoS One 2014; 9:e110531-[PMID: 25329921].

52. Baharivand N, Zarghami N, Panahi F, Yazdan DGM, Mahdavi Fard A, Abas M. Relationship between vitreous and serum vascular endothelial growth factor levels, control of diabetes and microalbuminuria in proliferative diabetic retinopathy. Clin Ophthalmol 2012; 6:185–191-[PMID: 22331976].

53. Funatsu H. Risk evaluation of outcome of vitreous surgery for proliferative diabetic retinopathy based on vitreous level of vascular endothelial growth factor and angiotensin II. Br J Ophthalmol 2004; 88:1064-8. [PMID: 15258026].

54. Yenihayat F, Özkan B, Kasap M, Karabaş VL, Güzel N, Akpınar G, Pirhan D. Vitreous IL-8 and VEGF levels in diabetic macular edema with or without subretinal fluid. Int Ophthalmol 2019; 39:821-8. [PMID: 29524030].

55. Sonmez K, Drenser KA, Capone A, Trese MT, Capone A Jr, Trese MT. Vitreous levels of stromal cell-derived factor 1 and vascular endothelial growth factor in patients with retinopathy of prematurity. Ophthalmology 2008; 115:1065-1070. e1. [PMID: 18031819].

56. Ehlken C, Rennel ES, Michels D, Grundel B, Pielen A, Junker B, Stahl A, Hansen LL, Feltgen N, Agostini HTHT, Martin G. Levels of VEGF but not VEGF165b are Increased in the

Vitreous of Patients With Retinal Vein Occlusion. Am J Ophthalmol 2011; 152:298-303.e1. [PMID: 21621189].

57. Taddei A, Giampietro C, Conti A, Orsenigo F, Breviario F, Pirazzoli V, Potente M, Daly C, Dimmeler S, Dejana E. Endothelial adherens junctions control tight junctions by VE-cadherin-mediated upregulation of claudin-5. Nat Cell Biol 2008; 10:923-34. [PMID: 18604199].

Articles are provided courtesy of Emory University and the Zhongshan Ophthalmic Center, Sun Yat-sen University, P.R. China. The print version of this article was created on 28 April 2021. This reflects all typographical corrections and errata to the article through that date. Details of any changes may be found in the online version of the article.